THE ASTROPHYSICAL JOURNAL, 281:535–544, 1984 June 15

SPECTROSCOPY OF THE NEBULOSITY AROUND EIGHT HIGH-LUMINOSITY QSOs

TODD A. BOROSON
Mount Wilson and Las Campanas Observatories, Carnegie Institution of Washington

AND

J. B. OKE
Palomar Observatory, California Institute of Technology
Received 1983 September 19; accepted 1983 December 12

ABSTRACT

Spectra between λ5000 and λ9500 have been obtained for the nebulosities around eight QSOs. These QSOs are all radio sources and were chosen for their high optical luminosities. The spectra of the nebulosities show either blue continua and strong emission lines or red continua with weak or no emission lines. We argue that all the continua arise from stars, although only one object, 3C 48, shows definite stellar absorption lines. Those objects showing strong emission lines require several times 10^8 solar masses of gas within the underlying galaxy. The separation into the two groups correlates with many other properties of the QSOs, including radio morphology and spectral index, Fe II emission, and Balmer line width.

Subject headings: galaxies: structure — interstellar: matter — quasars

I. INTRODUCTION

Although it is now generally recognized that most if not all low-redshift QSOs are surrounded by some sort of nebulosity, the precise nature of this extended material remains a mystery. Many imaging studies (Kristian 1973; Wyckoff, Wehringer, and Gehren 1981; Hutchings, Crampton, and Campbell 1984; Gehren *et al.* 1984; Malkan, Margon, and Chanan 1984) have claimed that the sizes, shapes, luminosities, and colors of the fuzz are consistent with their being galaxies. There is no consensus, however, on the types of galaxies involved, with everything from first-ranked giant ellipticals to low-luminosity spirals proposed. Certainly it is possible that a variety of different kinds of galaxies are involved. The situation is further complicated by analogies with other similar types of objects. For instance, Seyfert nuclei are thought to occur predominantly in spiral galaxies, while radio galaxies with classical double morphology are believed to be exclusively bright ellipticals.

The importance of understanding the relation between QSOs and their "host" galaxies lies in its implications both for the formation of QSOs and for the evolution of galaxies. The following questions outline the areas which might be attacked with information about the underlying galaxies in QSOs:

1. Are there correlations between QSO properties, such as luminosity, time scale for variability, and spectroscopic appearance, and galaxy properties, such as mass, angular momentum, and gas fraction? If such correlations exist, do they indicate the initial conditions necessary for the formation of a QSO, or for the fueling of a QSO over a longer period of time? Note that this question is related to the classification problem, since one must ask if there are intrinsic differences among the various active nuclei objects such as Seyfert galaxies, N galaxies, radio galaxies, BL Lac objects, and QSOs?

2. Can QSOs be used for cosmological investigations with the help of "host" galaxy information, either by limiting the sample on the basis of galaxy properties or by correcting measurements on the basis of correlations between QSO and galaxy properties? Alternatively, can the underlying galaxies be used as standard candles or standard yardsticks?

3. What are the effects on a galaxy of a QSO in the nucleus? Could the presence of the QSO be linked to any of the other energetic processes (star formation, galactic winds) which are known to be important in the evolution of a galaxy?

Assuming that the nebulosities around QSOs are in fact galaxies, the properties that one might hope to measure are the total luminosity of the underlying object, the distribution of luminosity (the morphology), and the specific features in the spectrum. While imaging studies, particularly those done with linear area detectors (Tyson, Baum, and Kriedl 1982; Gehren *et al.* 1984), unquestionably provide the best measurements of total luminosity and surface brightness distribution, spectroscopic investigations are also important. Spectroscopic observations are required to determine the relative contributions of gas and stars to the overall brightness, as well as the stellar population information needed to convert a total luminosity into a total mass. Spectroscopic studies also provide the only data on influences of the QSO upon the outlying material in terms of kinematic effects, photoionization, shock induced ionization or star formation, etc.

During the past several years, we have been obtaining spectra of the regions around a wide variety of QSOs with the double spectrograph on the Hale 5 m telescope. These observations have already led to the detection of an early-type stellar spectrum in the fuzz around the QSO 3C 48 (Boroson and Oke 1982). In this paper, we report on spectroscopic observations of the nebulosity around eight objects chosen for their high optical luminosity and as bright radio sources. These are, with one exception, all 3C or 4C radio sources, and all have luminosities brighter than $M_V = -24.4$. Table 1 lists the objects we have observed together with information about their general properties. The fuzz in several of these objects has been studied previously. These earlier studies are referred to later with reference to each object.

TABLE 1

THE SAMPLE OF HIGH-LUMINOSITY RADIO QSOS

Object (1)	z (2)	Scale (3)	V (4)	M_V (5)	log (F_{rad}) (6)	$\alpha(6, 20)$ (7)	Integration Time: Nucleus (8)	Integration Time: Fuzz (9)	Offset: Distance (10)	Offset: P.A. (11)
3C 48	0.367	6.2	16.2	−25.7	27.96	−0.75	1000	6000	2.0	0, 180
3C 249.1	0.311	5.6	15.7	−25.8	27.04	−0.90	2000	8000	2.0	135
3C 273	0.158	3.6	12.9	−27.1	28.48	+0.02	100	3000	3.0	90
4C 37.43	0.371	6.2	15.5	−26.4	26.85	−0.78	4000	12000	2.5	90, 270
3C 323.1	0.264	5.1	16.7	−24.4	27.04	−0.64	1000	4000	2.0	270
PKS 2141+174	0.213	4.4	15.5	−25.1	26.68	+0.20	1000	8000	2.0	45, 224
4C 31.63	0.297	5.5	15.5	−25.9	27.50	+0.02	2000	12000	2.0	135, 225, 315
4C 11.72	0.323	5.7	15.8	−25.8	26.96	−0.77	500	4000	2.5	270

EXPLANATION OF COLUMNS.—Col. (1) Name of object. Col. (2) Redshift of object. Col. (3) Angular to linear scale conversion factor (kpc per arcsecond) for $H_0 = 50$ and $q_0 = \frac{1}{2}$. Col. (4) Apparent V magnitude of QSO (from Hewitt and Burbidge 1980). Col. (5) Absolute V magnitude of QSO for $H_0 = 50$ and $q_0 = \frac{1}{2}$. Col. (6) Logarithm of the 6 cm radio (W Hz^{-1}) from Kuhr *et al.* (1981). Col. (7) Spectral index between 6 and 20 cm. Col. (8) Total integration time (s) for spectrum of nucelus. Col. (9) Total integration time (s) for spectrum of nebulosity. Col. (10) Distance in arcseconds offset from nucleus to obtain fuzz spectrum. Col. (11) Position angle or angles (north through east) of direction of offset to obtain fuzz spectrum.

II. THE OBSERVATIONS

The observations presented in this paper were made on eleven nights between 1981 November 4 and 1983 April 10 with the red side of the double spectrograph on the Hale 5 m telescope. The detector used was an 800 × 800 TI CCD with a readout noise of approximately 10 electrons. Spectra were obtained with a dispersion corresponding to 6.05 Å per pixel. With the 2″ slit used, the resolution is approximately 2.5 pixels. The spectra covered the wavelength range $\lambda\lambda$5000–9500. For each of the eight objects, both nuclear (QSO) spectra and off-nuclear (fuzz) spectra were obtained. The off-nuclear spectra were obtained by offsetting the spectrograph slit 2″ or 3″ from the QSO. The direction of the offset was chosen to maximize the surface brightness of the fuzz light through the slit, either by using the appearance of the object on the acquisition TV screen or by using published information about the morphology of the objects. If neither of these sources provided information, we rotated the spectrograph such that the direction of atmospheric dispersion was along the slit, and we offset perpendicular to this direction. Typical exposure times for a single integration were 1000 s for the observations centered on the QSO and 3000 s for those centered on the fuzz. For some of the objects we obtained as many as five separate integrations which were co-added after being reduced independently. The details of the observational material are presented in Table 1.

The spectra were first reduced in the usual way to one-dimensional arrays of sky-subtracted counts. They were calibrated to wavelengths using He-Ar comparison spectra taken after each exposure. They were then corrected for atmospheric extinction. Spectrophotometric standard stars were observed each night, and these were used to produce an array of corrections for atmospheric absorption features such as the *A* and *B* bands. These corrections were applied to each object spectrum. In most cases, this procedure removes the *B* band and the weak H_2O absorption features quite well. At the position of the *A* band, a residual spike often remains, because of the great depth of this feature. The standard star observations were then used to calibrate the QSO and fuzz spectra to approximate fluxes. Finally, all the individual QSO and fuzz spectra were co-added for each object, and the wavelength scales were converted to those of the rest frames of the objects.

Because of the effects of seeing and scattering, both in the atmosphere and at the mirror surfaces, all of the fuzz spectra show some contamination from the nearby QSOs. If the amount of this scattered light were constant with wavelength, it would be a fairly straightforward procedure to remove it, but atmospheric refraction and scattering effects cause it to vary with wavelength. Thus, some of the fuzz spectra are badly contaminated at the blue end and some at the red end. Those spectra for which we were able to orient the slit along the direction of atmospheric dispersion show fairly constant contamination. Therefore, we developed the following empirical technique for removing this light. Our first guess at the scattering spectrum (the fraction by which the QSO spectrum must be multiplied and subtracted) was simply taken from the ratio of the fuzz to QSO spectrum. That is, we assumed that little or no continuum was contributed by the fuzz and fit a low-order polynomial to the divided continuum level. This guess was applied by multiplying the scattering spectrum by the QSO spectrum, subtracting this result from the fuzz spectrum, and inspecting the result. We then improved the guess by judging at what wavelengths the QSO was over- or undersubtracted, modifying our polynomial in accordance with this, and recomputing the intrinsic fuzz spectrum. We stopped iterating when we could not significantly improve the appearance of the resulting spectrum. Thus, we tried to produce a final fuzz spectrum in which the mean continuum level does not go below zero, and in which the emission lines arising in the QSO (broad Balmer lines, Fe II lines, and He I λ5876) have been completely removed. Although our correction procedure is purely empirical, we were able to satisfactorily remove the scattered QSO light in most cases. The polynomials which we eventually derived for the scattering spectra were typically third- or fourth-order curves with minima near the center. The amplitude of the scattering was usually enough that about half of the light in our raw fuzz spectra was actually scattered from the nuclear regions. Individual objects will be discussed below. Figures 1 and 2 show the QSO spectra plotted as AB magnitudes against wavelength in the rest frame of the objects. Figures 3 and 4 show the fully corrected fuzz spectra plotted as flux per frequency interval against rest wavelength. The positions of the atmospheric *A* and *B* bands are indicated for each spectrum.

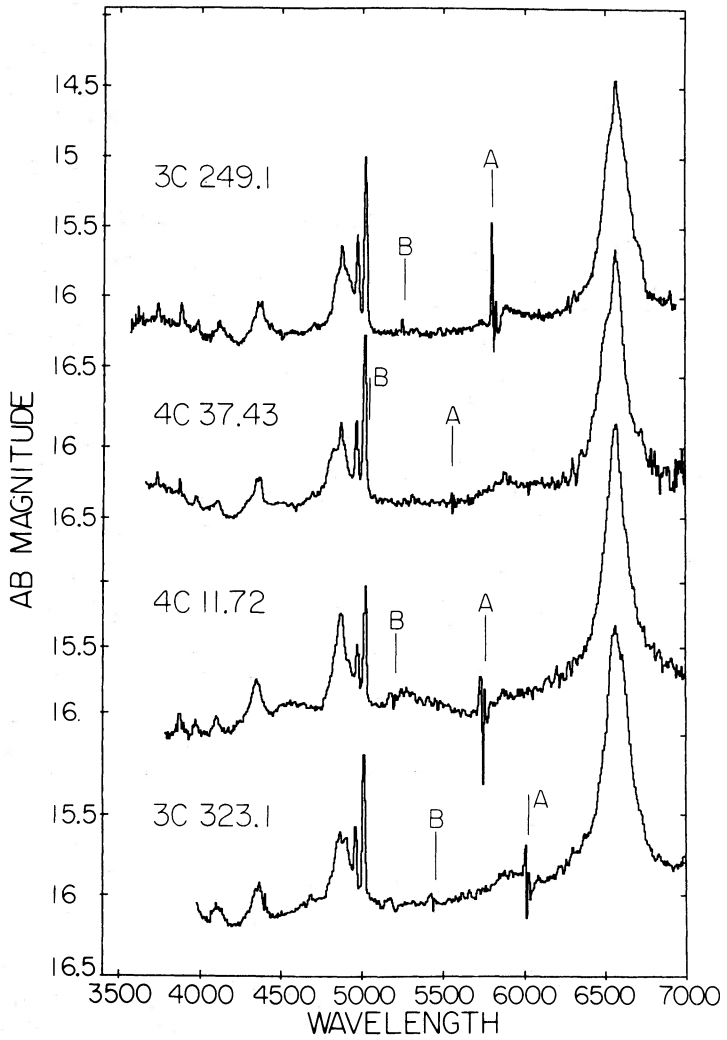

FIG. 1.—Spectra of the nuclei of four of the QSOs observed. The vertical scale is *AB* magnitudes, and the horizontal scale is wavelength in the rest frame of the QSOs. The positions of the telluric *A* and *B* bands are indicated.

III. THE FUZZ SPECTRA

It can be seen that the fuzz spectra range from those dominated by narrow emission lines (i.e., those in Fig. 3) to those with weak or no emission lines (Fig. 4). All of the spectra appear to have some continuous emission; the objects with redder continuum colors are those with weaker emission lines. None of the spectra with easily identified features show significant velocity differences from the nuclear spectra. We caution that due to the observing and reduction procedures, the precision of the velocities is only several hundred kilometers per second. Thus, we can say nothing about small redshift discrepancies between the nucleus and outer parts of the nebulosity caused by outflow, infall, rotation, etc.

We have measured the fluxes of all the observed emission lines, and these are given in Table 2. It should be emphasized that these fluxes are measured through a 2″ slit, and because of intensity gradients, in the objects are susceptible to wavelength-dependent losses caused mainly by refraction. This table also gives the monochromatic magnitude of the continuum of the fuzz at $\lambda 5500$ and a crude $B-V$ color measured from the spectrum for each object. Below, we describe the individual spectra.

3C 249.1.—The fuzz around this object was studied by Richstone and Oke (1977), who found evidence for emission lines from [O II], [O III], [Ne III], and possibly Hβ. Our spectrum (Fig. 3) confirms the presence of these emission lines, and adds Hγ, Hα, [O I] $\lambda 6300$, and the [S II] lines $\lambda\lambda 6716$, 6731 to the list. The $\lambda 3968$ line of [Ne III] is also visible in our spectrum in addition to the $\lambda 3869$ line seen by Richstone and Oke. Although we have not resolved the [N II] $\lambda\lambda 6548$, 6583 lines from Hα, the width of the Hα line and the presence of a bump on the redward side suggest that the [N II] lines may contribute as much as one-third to the observed emission in that complex.

Besides the emission lines, it is clear that a continuum is present. This cannot be residual scattered light from the QSO as a comparison with the QSO spectrum in Figure 1 shows that there is no evidence for the broad Balmer lines in the corrected fuzz spectrum. No absorption features are visible in the continuum, but this is not surprising considering its faintness. We shall argue below that the continuum present in all the objects must be due to stars.

4C 37.43.—This object was studied by Stockton (1976) who found emission lines of [O II], [O III], [Ne III], and [Ne V], as

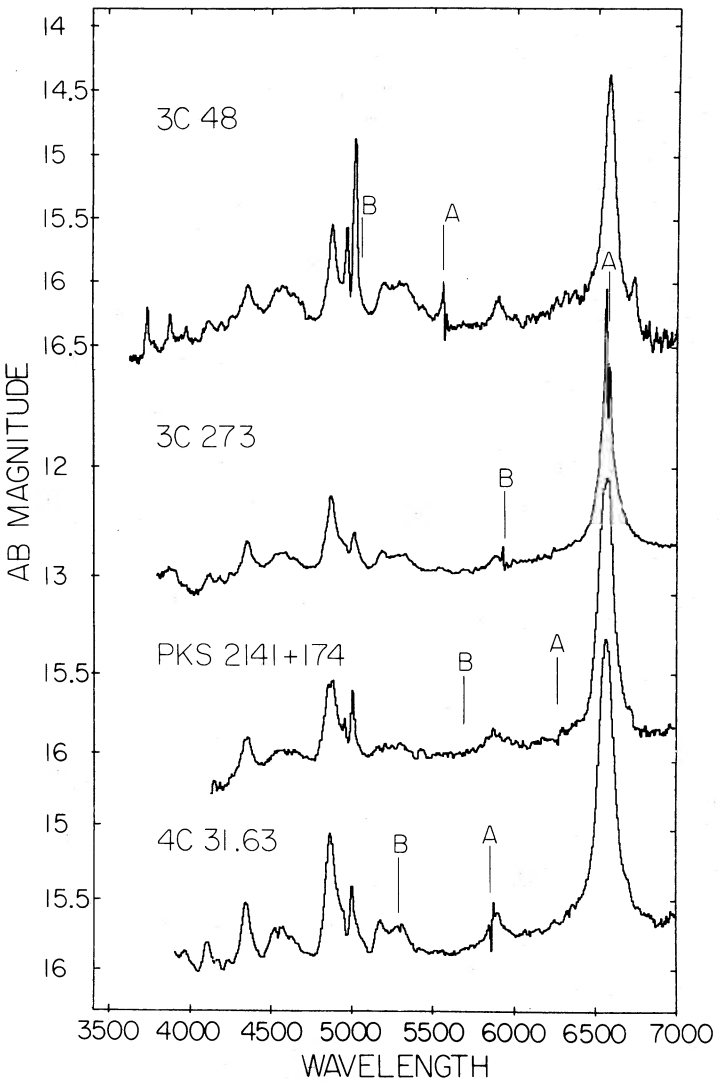

FIG. 2.—As Fig. 1 for the other four QSOs

TABLE 2

MEASURED AND CALCULATED PROPERTIES OF THE NEBULOSITIES

Property	3C 48	3C 249.1	3C 273	4C 37.43	3C 323.1	2141+175	4C 31.63	4C 11.72
AB_{5500}[a]	20.0	21.3	19.6	21.2	20.1	21.6	20.9	20.8
$B-V$	0.41	0.21	1.11	0.63	0.39	0.90	0.69	0.35
log F_{5007}[c]	41.60	43.01	42.34	42.88	42.48	<39.77	<40.04	42.73
f_{3727}[d]	3.8	16.	...	9.6	...	...	...	...
f_{3869}[e]	...	4.9	...	3.9	...	...	...	...
$f_{H\gamma}$[f]	...	3.2	...	1.8	...	...	...	...
f_{4363}[g]	...	1.2	...	0.9	...	...	...	...
f_{4686}[h]	...	...	...	0.9	...	...	...	...
$f_{H\beta}$[i]	...	7.4	...	4.3	4.3	...	...	4.1
f_{4959}[j]	0.9	24.	9.5	14.	10.	...	...	12.
f_{5007}[k]	2.3	72.	31.	44.	25.	...	...	36.
$f_{H\alpha+N\,II}$	...	35.	57.	21.	42.	3.5	...	27.
$f_{[S\,II]}$	8.6	9.9	4.6	3.2	...	...	8.6	...
M_V (gal)[n]	−24.4	−22.7	−22.8	−23.2	−23.5	−21.5	−23.4	−23.2

[a] Monochromatic AB magnitude at λ5500 ($AB = -2.5 \log f_\nu + 48.60$, where f_ν is in ergs s^{-1} cm^{-2} Hz^{-1}).
[b] $B-V$ color measured from spectrum.
[c] Logarithm of absolute flux of [O III] λ5007 in ergs s^{-1}.
[d–m] Observed flux of emission lines in units of 10^{-16} ergs s^{-1} cm^{-2}. Lines are as follows: [d] [O II] λ3727, [e] [Ne III] λ3869, [f] Hγ, [g] [O III] λ4363, [h] He II λ4686, [i] Hβ, [j] [O III] λ4959, [k] [O III] λ5007, [l] Hα + [N II] $\lambda\lambda$6548, 6583, and [m] [S II] $\lambda\lambda$6716, 6731.
[n] Extrapolated total absolute visual magnitude of the underlying galaxy. Slit is assumed to have subtended one-tenth of light from entire galaxy.

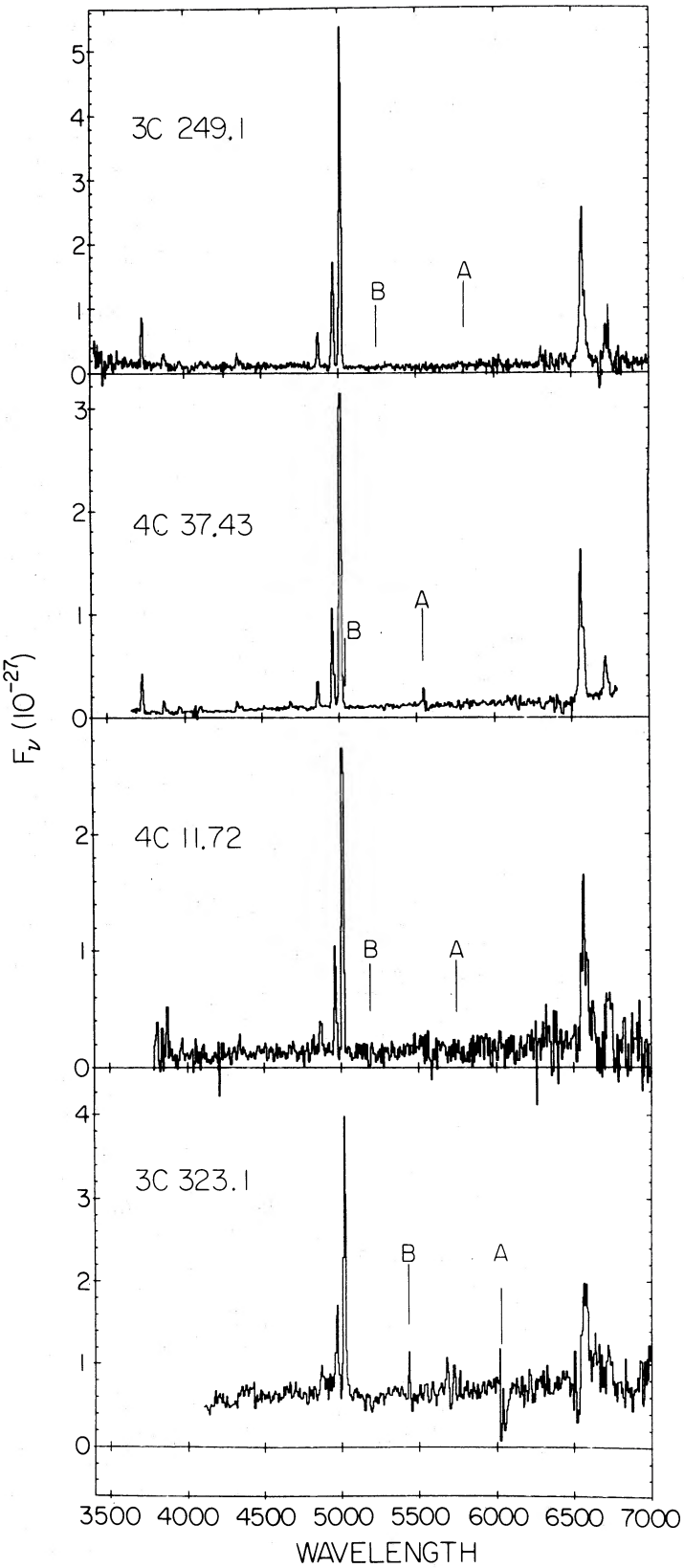

FIG. 3.—Spectra of the nebulosity around four of the QSOs observed. Note that these are the same objects in the same order as the nuclear spectra in Fig. 1. These are the objects with emission-line-dominated fuzz. The positions of the telluric *A* and *B* bands are indicated.

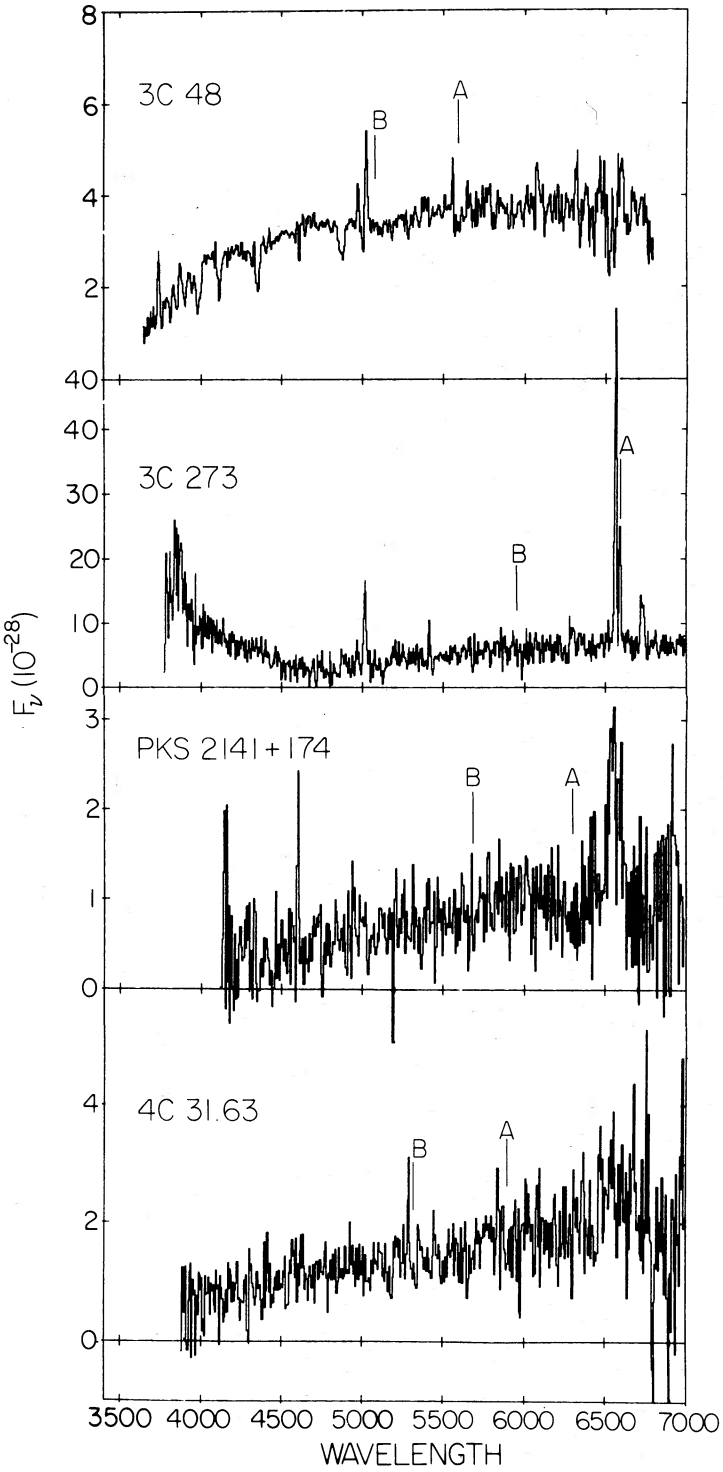

FIG. 4.—Spectra of the nebulosity around four of the QSOs observed. Note that these are the same objects in the same order as the nuclear spectra in Fig. 2. These are the objects with continuum-dominated fuzz. The positions of the telluric *A* and *B* bands are indicated.

well as narrow Balmer lines in the spectrum of the fuzz. Our spectrum shows these lines, with the exceptions of [Ne v] λ3426, which is shortward of our spectral coverage, and [O III] λ4363. He II λ4686 is clearly present in our data. Further to the red, we see Hα and the [S II] lines. The continuum level in this object is somewhat larger than in 3C 249.1, and the continuum appears slightly redder, although we hesitate to draw conclusions about the intrinsic color because of atmospheric refraction and scattered light uncertainties. No absorption features are seen in the continuum; in particular, the Mg I *b* band and the λ4000 break are not present.

4C 11.72.—This spectrum, although much noisier, is quite similar to those of 3C 249.1 and 4C 37.43. The Hβ, [O, III] $\lambda\lambda$4959, 5007, Hα, and [S II] lines are all easily seen. The wavelength coverage does not extend far enough to the blue to see λ3727, but there is a possible weak emission feature at the position of [Ne III] λ3869. As in the previous two objects, the continuum is blue.

3C 323.1.—This is one of the objects studied by Miller (1981) in his attempt to detect diluted stellar absorption features in the nuclear spectra of QSOs. His conclusion was that any underlying galaxy is contributing less than 10% of the light from this object. Of course, the approach used by Miller presupposes that the dominant features will be those commonly associated with old stellar populations. Our spectrum of the nebulosity around 3C 323.1 shows a moderately strong continuum with emission lines of Hβ, [O III] $\lambda\lambda$4959, 5007, Hα, and [S II] $\lambda\lambda$6716, 6731. Weak absorption may be present at the positions of the *G* band (λ4300) and the Mg I *b* band (λ5170), but the sky subtraction for this object is poor, and we are not certain of the reality of these features.

3C 48.—Our observations of 3C 48 were first reported in Boroson and Oke (1982); the spectrum shown in Figure 4 is a composite made from those data. In addition to the strong Balmer absorption features and emission lines of [O II] and [O III], the continuum shape suggests that *G* band and Mg I *b* band absorption are present in the stellar population. This QSO remains unique in terms of the spectral appearance of its nebulosity. The $B-V$ color of this continuum (0.41) is indicative of early F stars, though the spectral appearance suggests a mix of types earlier and later than this.

3C 273.—Imaging and spectroscopic observations of the fuzz around this very luminous QSO were reported by Wyckoff *et al.* (1980). These authors detected a 15″ radius nebulosity with a total absolute magnitude in the *R* band of -25. This detection was confirmed by Tyson, Baum, and Kreidl (1982), who argued on the basis of the underlying objects total luminosity and radial profile that it was very similar to a first-ranked elliptical galaxy in a rich cluster. The spectroscopy presented by Wyckoff *et al.* (1980) was not conclusive; they found weak [O II] λ3727, [O, III] λ5007, and [Ne III] λ3869 emission lines but were unable to directly observe the continuum.

The brightness of the nucleus of this object makes the observations of the nebulosity somewhat more difficult than any of the other objects. Furthermore, a problem with frost in the red camera plagued our observations of this object to a much greater extent than those of any other. Thus, although we accumulated a total of about 15,000 s of integration time on the fuzz around 3C 273, we show in Figure 4 our best 3000 s spectrum. Addition of any of the other spectra we obtained seemed only to degrade the signal-to-noise ratio of the result. The blue turnup below λ4500 is a residual artifact of the scattered nuclear light removal. The red continuum longward of this is real, as are the emission lines of [O III], [O I] λ6300, Hα, and the [S II] lines. Note that in this object the atmospheric *A* band falls in the middle of Hα; thus, this produces the double structure seen in the line and some uncertainty as to its total intensity. A slight dip above λ5100 is suggestive of the presence of the Mg I *b* band in the nebulosity, but the spectrum is really too noisy to say for sure.

PKS 2141+174.—This QSO (also known as OX 169) has been imaged by Hutchings, Crampton, and Campbell (1984) and by Gehren *et al.* (1984). Both groups resolve its extended structure and mention a jetlike extension on the southeast side. The red continuum in this nebulosity is the faintest of any we observed. Hα appears in emission, and we trust the reality of this feature since, were we to subtract a larger contribution from the nucleus, the continuum on either side of the emission line would be depressed. This emission line is the only convincing feature, although the general continuum shape suggests the presence of MgH absorption.

4C 31.63.—This QSO has been resolved by Hutchings, Crampton, and Campbell (1984) who find a very luminous underlying galaxy. Our spectrum shows no strong features in either absorption or emission. A sharp absorption feature at λ5180 might be due to Mg I, but the absence of the broad MgH dip which usually accompanies this line makes this identification uncertain.

IV. DISCUSSION

a) The Emission Lines

Without computing detailed models, a few interesting conclusions can be drawn from the strengths of the emission lines. This analysis applies primarily to those objects (in Fig. 3) in which the emission lines dominate the spectrum. The large ratio of the strengths of the [O III] $\lambda\lambda$4959, 5007 lines to that of Hβ, in combination with the presence of reasonably strong [O II] λ3727, implies photoionization by a power-law source. This conclusion was previously reached for 3C 48 by Wampler *et al.* (1975), for 4C 37.43 by Stockton (1976), and for 3C 249.1 by Richstone and Oke (1977).

In the four objects in which both Hα and Hβ are detectable, the ratio of Hα to Hβ is too large for simple recombination. This may be due to (*a*) our inability to resolve and exclude the [N II] lines from either side of Hα, (*b*) poor signal-to-noise ratio at Hα from unsuccessful subtraction of night sky and nuclear region features, (*c*) radiative transfer effects, and (*d*) reddening within the galaxy. The blending of Hα and the [N II] lines is certainly an important consideration in 3C 249.1, 4C 37.43, and 4C 11.72. In these objects the apparent widths of the blend and secondary peaks corresponding to the [N II] lines indicate that as much as one-third of the flux in the complex is actually due to the [N II] lines. A further complication is caused by atmospheric refraction, because of which somewhat different regions in the nebula might be seen at two ends of the spectra. The fact that the scattered light from the nucleus was not constant with wavelength supports this possibility.

It is of particular interest to estimate the quantity of gas required to produce the observed emission lines. The two objects in which [O III] λ4363 is seen give electron temperatures (T_e) of about 15,000 K (for $N_e < 10^4$) from the ratio of this line to [O III] $\lambda\lambda$4959, 5007. We adopt this value for further calculations. The electron density is more difficult to determine.

In 3C 249.1, the [S II] $\lambda\lambda$6716, 6731 lines are clearly separated and have a ratio of about 1.2 in favor of the λ6716 line. This gives an electron density (N_e) of 500 cm^{-3}. In the other objects which show the [S II] lines the relative intensities are uncertain, but the λ6716 line appears stronger in all cases. This indicates an upper limit of about 1000 cm^{-3} for the electron densities. The ratio of the two [S II] lines asymptotically approaches about 1.4 as the density decreases so, given the uncertainties in the observations of the lines, an electron density much smaller than the numbers mentioned is quite possible.

The Hβ flux, together with the electron temperature, allows us to derive $N_e^2\ V$ of 1.28×10^{67} and 8.9×10^{66} for 3C 249.1 and 4C 37.43, respectively. These two objects have the strongest emission-line fluxes. These values correspond to $1.1 \times 10^{10}\ N_e^{-1}$ and $7.5 \times 10^9 N_e^{-1}\ M_\odot$ of material *in the region we observed*. For $N_e = 500$ cm^{-3} and with the assumption that our slit subtended about 10% of the nebula, 2.2×10^8 and $1.5 \times 10^8\ M_\odot$ are the total gas masses for 3C 249.1 and 4C 37.43, respectively. The only lower limit to the electron density comes from assuming the entire region we observed is uniformly filled with gas. The volume of this region is about 10^{68} cm^3. This volume implies an electron density (from the $N_e^2\ V$ value for 3C 249.1) of 0.3 cm^{-3} and a total mass of $3.2 \times 10^{11}\ M_\odot$.

b) *The Continua*

Table 2 lists for each object an observed monochromatic magnitude at λ5500 and a $B-V$ color measured from the final spectra. It should be noted that even the objects which have spectra dominated by emission lines have detectable continua. As was argued in Boroson, Oke, and Green (1982), it is hard to imagine that this continuous emission could be anything but starlight. In particular, scattered light is ruled out by the absence of the broad nuclear emission lines, and any combination of bound-free and free-free emission from the gas is ruled out by the small equivalent width of Hβ.

Given that this is starlight, the measured $B-V$ colors for the continua suggest the presence of early-type stars in some of the spectra. The four objects dominated by emission lines (and also 3C 48) have continuum colors consistent with their being young populations. For comparison with the $B-V$ colors presented in Table 2, spiral galaxies have total face-on colors ranging from 0.70 to 0.45 along the sequence Sa to Scd (de Vaucouleurs 1977). Although these blue colors may suggest that some of the underlying galaxies are spirals, it should be remembered that the presence of the QSO in the nucleus of each of these objects might cause a peculiar star formation history. For example, the $B-V$ color of the active elliptical NGC 1275 is 0.52 (de Vaucouleurs, de Vaucouleurs, and Corwin 1976), almost as blue as these objects. The remaining three objects, 3C 273, PKS 2141+174, and 4C 31.63, have much redder continua. Their colors are easily compatible with the $B-V$ colors of typical old populations as are found in elliptical galaxies.

The absence of obvious absorption features also supports the conjecture of early-type stars in some of the spectra. Certainly, if the 4C 37.43 continuum consists of late type stars, the Mg I *b* band would be easily visible in a spectrum of this quality. As a quantitative estimate of the possible contribution from an old stellar population, we calculated the Mg_2 line index (Faber, Burstein, and Dressler 1977) for several of the objects. This line index measures the strength of both the atomic Mg I triplet and the broad molecular MgH absorption. Its value in magnitudes ranges from about 0.25 to 0.35 in elliptical galaxies (Terlevich *et al.* 1981). In 4C 37.43, the measured value of the Mg_2 index is 0.098, confirming our impression that late-type stars are contributing only a small fraction (no more than about 30%) of the continuum. 3C 249.1 and 3C 31.63 have Mg_2 values of 0.315 and 0.221, respectively. The continua are somewhat noiser in these objects, however, and we are unsure of the significance of the apparent absorption, particularly in the light of the blue colors discussed above. 3C 48 has a Mg_2 value of 0.058, suggesting about 20% of the continuum light may be coming from a late-type population. 4C 31.63 has a Mg_2 value of 0.344, consistent with a pure, late-type population. The other three objects, 3C 273, 4C 11.72, and PKS 2141+174, have continua too noisy to determine believable Mg_2 indices.

One implication of the colors of the continua is their relation to the mass-to-light ratio (M/L) of the underlying galaxies. This is relevant to studies which attempt to quantify the total masses and luminosities of the galaxies in which QSOs form. Since there is so much variation in color among the objects, corrections should be applied to the luminosities in order to derive a measure of the mass of the object independent of M/L. The difference between the M/L of a population with a $B-V$ color of 0.45 and one of 0.95 can be a factor of 10 or 2.5 mag (Larson and Tinsley 1978).

In the light of the continuum magnitudes and colors, we next inquire whether our measurements are consistent with the premise that QSOs form in first-ranked giant elliptical galaxies. To do this, we make the assumption (identical to that made when we considered the emission line fluxes) that our slit subtends one-tenth of the light from the underlying galaxy (Boroson, Oke, and Green 1982). We can then compare a ranked giant elliptical ($\langle M_V \rangle = -23.26$; Sandage 1972) at the redshift of each of the QSOs with the extrapolated absolute magnitudes of the observed nebulosities. These absolute magnitudes are presented in the bottom row of Table 2 [labeled M_V (gal)]. Comparison of these numbers with the value of -23.26 shows the relative total *visual* luminosities of the underlying galaxies to a first-ranked giant elliptical. For 3C 273, 4C 31.63, and PKS 2141+174, which have red continua, there is clearly no problem in attributing the light to a bright elliptical galaxy population. For the other group of objects with blue continua and strong emission lines, the colors are too blue to permit large contributions from an old population. The luminosity is, however, consistent with the fuzz being a luminous galaxy with younger populations of stars. In the case of 3C 48 which has already been discussed (Boroson and Oke 1981), this young population produces an abnormally luminous galaxy, although the mass is almost certainly normal.

c) *The Two Groups of Objects*

The most striking thing about the fuzz spectra in Figures 3 and 4 is the separation into those dominated by emission lines and those dominated by continuum. It was on this basis that the objects were divided into the two figures, but, in fact, this separation correlates with some of the other properties of the objects.

We first noticed that the emission-line-dominated objects (hereafter blue fuzz objects) all had steep radio spectra and the continuum-dominated objects (hereafter red fuzz objects) had flat spectra. 3C 48 is an exception to this; it has a steep radio spectral index, but its compact radio morphology is

much more typical of the flat spectra sources. Also, inspection of the nuclear spectra shows that the blue fuzz objects tend to have much stronger [O III] lines than the red fuzz objects, whereas the red fuzz objects all have strong Fe II emission (the broad bands on either side of the Hβ, [O III] complex), and the blue fuzz objects do not. Finally, the Balmer lines in the blue fuzz objects are in the mean about 50% broader and have equivalent widths about 20% larger than the red fuzz objects.

Several previous studies have attempted to classify QSOs and active galactic nuclei on the basis of these and other measurable properties. Setti and Woltjer (1972) and Schmidt (1976) separated the flat spectrum radio source QSOs from the steep spectrum radio source QSOs. Both of these studies found that the V/V_m test indicated that the flat spectrum objects showed much less cosmological evolution than the steep spectrum objects. This finding has been disputed by other studies (Blake 1978; Peacock *et al.* 1981). Miley and Miller (1979) separated low-redshift QSOs by their radio morphology. They found that the extended structure QSOs (generally steep spectrum objects) had broader optical emission lines than the compact structure QSOs (generally flat spectrum objects). They also found that the compact structure QSOs more frequently showed strong Fe II emission. Steiner (1981) classified QSOs and active nuclei on the basis of the strength of their Fe II emission. He found that the objects with Fe II emission are radio quiet or have flat spectra and compact structure, while the objects with no Fe II emission have steep spectra and extended structure. He found that the Fe II emitters show a good anticorrelation between [O III]/Hβ and either optical or X-ray luminosity, while the objects without Fe II show no relation between these two quantities.

Clearly, all these studies (this one included) have found basically the same two groups of objects. We summarize the properties of the two groups of objects in Table 3.

It is likely that some very basic difference exists between these two groups of QSOs since such a large variety of properties are affected. In particular, the nuclear properties (as delineated by the broad emission lines and the radio morphology) are linked in some way to the spectrum of the nebulosity; presumably these differences between the two groups are all manifestations of some fundamental distinction between the objects in the two groups which must have to do with how quasars work.

d) Possible Explanations for the Two Groups

In terms of the fuzz, the obvious question is why the red fuzz objects do not show emission lines. Three possible reasons are (1) no ionizing radiation escapes the nucelus, (2) there is no gas in the fuzz, and (3) a peculiar geometry prevents the ionizing photons from reaching the fuzz or prevents us from seeing the emission lines. We address each of these explanations below.

TABLE 3

THE TWO CLASSES OF QUASI-STELLAR OBJECTS

Component of Quasar	Group 1	Group 2
Nebulosity	Blue continuum Strong emission lines	Red continuum Weak or absent emission lines
Nucleus, optical	No Fe II emission Narrow lines are strong Very broad, bumpy H lines [O III]/Hβ large	Strong Fe II emission Narrow lines are weak Less broad, smooth H lines [O III]/Hβ moderate
Radio source	Steep spectral index Double lobed structure	Flat spectral index Compact structure
Cosmological	More evolution (?)	Less evolution (?)

1. Two arguments suggest that it is not a lack of ionizing radiation which prevent emission lines from arising in the fuzz. First, although no objects with redshifts as small as those in our sample have been observed below the Lyman limit, the experience with higher redshift objects is that only a small fraction (about 10%) show significant absorption there. This has been attributed to small covering factors rather than low optical depth. It should be noted, however, that the possible difference in cosmological evolution between the two groups might cause a very much higher fraction of high-redshift objects to be blue fuzz objects rather than red fuzz objects. A more direct argument against the nucleus absorbing all the ionizing photons is the equivalent widths of the permitted lines. If the covering factor were high enough to completely enclose the continuum source in the red fuzz objects, the Hβ equivalent width would be expected to be larger by a factor approaching 10. This is clearly not the case; in fact, the Hβ equivalent widths are about 20% *smaller* in the red fuzz objects. Searle and Sargent (1968) showed that the fairly constant equivalent width of Hβ in extragalactic objects suggests that a uniform fraction of a power-law continuum is absorbed in these objects. It appears that roughly the same fraction (about 90%) of the ionizing radiation is escaping the nucleus in both types of objects.

2. A second possibility is that there is no gas in the outer regions of some of the host galaxies. Certainly, with the exception of 3C 48, the colors of the continua of the nebulosity are red enough to represent typical old stellar populations which might be expected to be devoid of gas. Moreover, the strength of the lines from the narrow line region surrounding the nucleus is much smaller than in the blue fuzz objects, suggesting a general deficiency of low density gas in these objects. It should also be recognized that BL Lacertae objects might represent an extreme member of the red fuzz group. They are flat spectral index compact radio sources and have fuzz dominated by late-type stellar continuum. They therefore represent objects with so little gas that even the broad nuclear emission lines cannot be produced.

There are two problems related to explaining the difference between the red fuzz objects and the blue fuzz objects in terms of the presence or absence of gas in the outer regions of the host galaxies. First, it must be recognized that there is at least enough gas present to provide the broad-line region. Second, as there is some current controversy over whether the host galaxies are spirals or ellipticals, it is tempting to speculate that the blue fuzz objects have nearby gas because they are in spirals while the red fuzz objects do not because they are in gasless elliptical galaxies. The difficulty with this interpretation is the fact that almost all powerful, steep spectrum, extended radio sources which are close enough for the optical morphology to be studied are in elliptical galaxies. This trend would be directly contradicted if the blue fuzz objects are in spiral galaxies. A related argument against this potential separation into spirals and ellipticals comes from Steiner's (1981) classification in which his Class A (our red fuzz) objects were predominantly found in underlying galaxies with spiral arms, while his Class B (our blue fuzz) objects were predominantly found in amorphous galaxies.

3. The final possibility we discuss is that the differences are a result of a geometry or orientation difference between the two classes of objects. An old application of this idea is that the comjact radio sources are simply extended sources seen from one end, along a relativistic jet. The main problem with this explanation is understanding the observed correlation between viewing angle and the emission line properties (see Heckman 1983). Our finding is that the connection is not only with the nuclear emission-line properties, but with the emission-line properties of the entire underlying object. This strengthens the argument against the observed differences being due to geometry or viewing orientation.

A more promising approach might be related to alignment of disks. Suppose two disks are involved in these objects, one an accretion disk around the central continuum source, the other a disklike distribution of gas in the host galaxy. If the two disks were well aligned in the red fuzz objects, the gas in the outer regions of the galaxy would be shadowed from the ionizing radiation by the accretion disk. This would explain both the lack of emission lines in these objects and the presence of Fe II emission which requires an extremely optically thick region in which to form. The blue fuzz objects might then have disks with different axes, or perhaps a much smaller or absent accretion disk, allowing the ionizing radiation out into the outer gas disk. This picture, of course, does not explain the radio properties or the variation in line width seen between the two groups. It is clear that an analysis involving the more easily measurable properties of many objects is desirable in order to sort out the physical differences between the two types of QSOs.

In summary, we have measured spectroscopically the nebulosity around eight QSOs chosen for their high luminosity. In addition, they are all radio sources, and the fuzz around several of them has been studied previously. We find that the appearance of the fuzz separates the objects into two groups. Half of the objects have fuzz dominated by blue continuous radiation and strong narrow emission lines. The remaining objects have fuzz which shows redder continua and weak or entirely absent emission lines. This separation into two groups is well correlated with many other observable properties such as radio spectral index and the presence of Fe II emission lines in the nuclear spectra. We are unable to come up with a satisfactory explanation for this dichotomy, but the connection between properties at so many scales suggests that the controlling factor is an important physical process in the central regions of QSOs.

We are pleased to thank J. Carrasco for assistance at the telescope. This work was partially supported by the National Science Foundation through grant AST-8215118.

REFERENCES

Blake, G. M. 1978, *M.N.R.A.S.*, **183**, 21P.
Boroson, T. A., and Oke, J. B. 1982, *Nature*, **296**, 397.
Boroson, T. A., Oke, J. B., and Green, R. F. 1982, *Ap. J.*, **263**, 32.
de Vaucouleurs, G. 1977, in *The Evolution of Galaxies and Stellar Populations*, ed. B. M. Tinsley and R. B. Larson (New Haven: Yale University), p. 43.
de Vaucouleurs, G., de Vaucouleurs, A., and Corwin, H. G. 1976, *Second Reference Catalog of Bright Galaxies* (Austin: University of Texas Press).
Faber, S. M., Burstein, D., and Dressler, A. 1977, *A.J.*, **82**, 941.
Gehren, T., Fried, J., Wehinger, P. A., and Wyckoff, S. 1984, *Ap. J.*, **278**, 11.
Heckman, T. M. 1983, *Ap. J.* (*Letters*), **271**, L5.
Hewitt, A., and Burbidge, G. R. 1980, *Ap. J. Suppl.*, **43**, 57.
Hutchings, J. B., Crampton, D., and Campbell, B. 1984, *Ap. J.*, **280**, 41.
Kristian, J. 1973, *Ap. J.*, (*Letters*), **179**, L61.
Kuhr, H., Nauber, U., Pauliny-Toth, I. I. K., and Witzel, A. 1981, *Astr. Ap. Suppl.*, **45**, 367.
Larson, R. B., and Tinsley, B. M. 1978, *Ap. J.*, **219**, 46.
Malkan, M. A., Margon, B., and Chanan, G. A. 1984, *Ap. J.*, **280**, 66.
Miley, G. K., and Miller, J. S. 1979, *Ap. J.* (*Letters*), **228**, L55.
Miller, J. S. 1981, *Pub. A.S.P.*, **93**, 681.
Peacock, J. A., Perryman, M. A. C., Longair, M. S., Gunn, J. E., and Westphal, J. A. 1981, *M.N.R.A.S.*, **194**, 601.
Richstone, D. O., and Oke, J. B. 1977, *Ap. J.*, **213**, 8.
Sandage, A. R. 1972, *Ap. J.*, **178**, 1.
Schmidt, M. 1976, *Ap. J.* (*Letters*), **209**, L55.
Searle, L., and Sargent, W. L. W. 1968, *Ap. J.*, **153**, 1003.
Setti, G., and Woltjer, L. 1973, *Ann. NY Acad. Sci.*, **224**, 8.
Steiner, J. E. 1981, *Ap. J.*, **250**, 469.
Stockton, A. 1976, *Ap. J.* (*Letters*), **205**, L113.
Terlevich, R., Davies, R. L., Faber, S. M., and Burstein, D. 1981, *M.N.R.A.S.*, **196**, 381.
Tyson, J. A., Baum, W. A., and Kriedl, T. 1982, *Ap. J.* (*Letters*), **257**, L1.
Wampler, E. J., Robinson, L. B., Burbridge, E. M., and Baldwin, J. A. 1975, *Ap. J.* (*Letters*), **198**, L49.
Wyckoff, S., Wehinger, P. A., and Gehren, T. 1981, *Ap. J.*, **247**, 750.
Wyckoff, S., Wehinger, P. A., Gehren, T., Morton, D. C., Boksenberg, A., and Albrecht, R. 1980, *Ap. J.* (*Letters*), **242**, L59.

TODD A. BOROSON: Mount Wilson and Las Campanas Observatories, 813 Santa Barbara Street, Pasadena, CA 91101

J. B. OKE: Department of Astronomy 105-24, California Institute of Technology, Pasadena, CA 91125